Profiling Intermolecular Interactions of Theophylline: Analysis of Some Classes of Theophylline Containing Co-Crystals

Martin H. Polko, Guido J. Reiss

Suggested Citation:
Polko, M. H., & Reiss, G. J. (2026). Profiling Intermolecular Interactions of Theophylline: Analysis of Some Classes of Theophylline Containing Co-Crystals. Crystals, 16(5), Article 342.
https://doi.org/10.3390/cryst16050342

crystals

MDPI

Article

Profiling Intermolecular Interactions of Theophylline: Analysis of Some Classes of Theophylline Containing Co-Crystals

Martin H. Polko and Guido J. Reiss *

Institut für Bioanorganische Chemie, Heinrich-Heine-Universität Düsseldorf, 40225 Düsseldorf, Germany; martin.polko@hhu.de

* Correspondence: reissg@hhu.de

Abstract

Intermolecular interactions play an important role in the formation and stability of co-crystals. In this study, the interaction behaviour of theophylline in co-crystal structures was systematically analysed using data from the Cambridge Structural Database. A total of fifty-three theophylline co-crystal structures were investigated and classified according to their intermolecular interaction motifs. A structured interaction scheme was developed to describe the accessible interaction sites of theophylline, including classical and non-classical hydrogen bonds, as well as halogen bonds and π···π interactions. The study revealed theophylline's high versatility in forming intermolecular interactions, resulting in twenty interaction patterns. Three dominant motifs were identified as occurring most frequently. The results indicate that steric effects influence the accessibility of specific interaction sites, particularly limiting interactions at the carbonyl group located between the two methyl groups. Hirshfeld surface analysis revealed that O···H and H···H interactions contribute most significantly to the intermolecular interactions in the analysed structures.

Keywords: crystal structure; weak interactions; hydrogen bonding; theophylline; crystal structure prediction

1. Introduction

Understanding the crystal structures of molecular compounds is a central challenge in Crystal Structure Prediction (CSP) [1]. The crystal packing of organic molecules is governed by a delicate balance of intermolecular interactions, including hydrogen bonding, π–π stacking, steric effects and many weak interactions that are weaker than hydrogen bonds. Because many possible arrangements can have very similar lattice energies, identifying the most stable or experimentally accessible crystal structures remains difficult. Nevertheless, reliable prediction of crystal structures is highly desirable, particularly in pharmaceutical science [2]. One strategy for improving CSP approaches is a systematic analysis of intermolecular interaction motifs in known crystal structures. Detailed structural analyses, including methods such as Hirshfeld surface analysis [3], allow for the quantitative characterisation of close contacts and interaction preferences in molecular crystals. Such information can help identify recurring supramolecular synthons and preferred binding sites, which may guide the prediction of packing motifs and co-crystal formation. The class of co-crystals is currently of great interest, as co-crystallisation enables the modification of many physical properties of a target compound [4–6]. Theophylline belongs to a class of compounds of active pharmaceutical ingredients (APIs). In the specific case of theophylline, co-crystal formation, X-ray diffraction studies and intermolecular interactions have already

Academic Editor: Aidar T. Gubaidullin

Received: 19 March 2026
Revised: 11 May 2026
Accepted: 14 May 2026
Published: 18 May 2026

been the subject of numerous studies. Previous work has focused on hydrogen bonding behaviour, supramolecular synthons, and the structural diversity of theophylline-based multi-component systems [7–12]. Despite these extensive studies, a systematic and unified classification of all relevant interaction types beyond classical hydrogen bonding is still limited. In particular, interactions such as π···π stacking, halogen bonding, and non-classical hydrogen bonds are often not considered within a single, consistent framework, making direct comparisons between different co-crystal systems difficult.

To address this lack of overview, the interaction behaviour of theophylline in co-crystals with different co-formers is systematically analysed in this work. Specific interaction sites involved in co-crystal formation are identified and the most frequent interaction patterns are examined. By correlating observed interaction patterns with structural constraints, this study contributes to the understanding of molecular recognition in theophylline co-crystals and provides insights that may support future crystal structure prediction and data-driven approaches to solid-state design. This study is part of our general interest in methylxanthines and in-detail research on theophylline [13], its salts [14,15], and caffeine-containing compounds [16], and extends these investigations towards a more comprehensive and comparative analysis of intermolecular interactions in co-crystals. The overall aim of this study is to identify the preferred interaction sites of theophylline co-crystals depending on the choice of co-crystal component.

2. Methodology

From the large number of crystal structures of co-crystals of theophylline with defined co-crystal components some specific groups were identified and extracted from the Cambridge Structural Database [17]. The selection of co-crystal structures was intended to be focused on representative systems that allow for a systematic comparison of intermolecular interactions. Co-crystal components were classified into three major classes: (i) aromatic compounds, enabling the investigation of π···π interactions; (ii) short carbon-chain molecules, which provide flexible systems with reduced steric hindrance; and (iii) components forming hydrate structures, allowing for the analysis of water-mediated interactions. In addition, the selected systems include a variety of functional groups to ensure a broad representation of potential hydrogen bond donors and acceptors, as well as other interaction types. It should also be noted that the dataset includes co-crystals with different stoichiometries as well as hydrate forms. These were not treated separately, as the focus of this study is on intermolecular interaction patterns rather than polymorphism or phase behaviour. This targeted selection enables a consistent and comparative analysis of interaction patterns across structurally diverse co-crystal systems. Consequently, not all reported theophylline co-crystals described in the literature were included. More complex systems, such as multi component pharmaceutical co-crystals or highly substituted co-formers, were excluded in those cases where their structural complexity would hinder a consistent classification within the applied framework. The focus of this study is therefore more on comparability rather than completeness. The complete list of all co-crystal components investigated is provided in the Supplementary Material. The subdivision of co-formers provided in the Supplementary Material is based on dominant functional groups and serves as a supporting classification for the structural analysis. It is not intended as a strict hierarchical scheme, but rather as a pragmatic grouping of chemically diverse systems. The intermolecular interaction patterns of all selected co-crystals structures were examined using the crystallographic software Mercury (Ver. 4.0), taking into account the atom distances and angles [18]. Based on this empirical analysis, the co-crystals were classified according to their dominant interaction motif. Dominance was defined based on the frequency and structural relevance of specific intermolecular interactions within

the crystal structure, taking into account their occurrence, geometric consistency, and role in forming extended supramolecular motifs. It should be noted that this classification is based on geometrical and topological criteria derived from crystallographic data and does not directly quantify interaction energies [13]. While cooperative effects between different interactions are inherently present in crystal structures, they are considered here in a qualitative manner through their contribution to the overall structural motif.

A schematic overview of most relevant interactions accessible to theophylline is presented in Figure 1, which represents a case-optimised version of other already existing illustrations [19,20]. In contrast to earlier approaches, this study not only includes classical hydrogen bonds, but also explicitly incorporates π···π interactions, halogen bonding, and non-classical hydrogen bonds. Hydrogen bond sites are labelled according to their molecular position. Theophylline is theoretically able to engage in four classical hydrogen bonds, which are labelled from **A**–**D** and coloured in red (O) or blue (N), depending on the acceptor atom. In addition, the purple indicated site **G** (C-H) can act as a non-classical hydrogen bond donor. π···π interactions, including π···π stacking between theophylline and other aromatic systems, as well as C=O···π interactions involving the carbonyl group of theophylline, are indicated in orange as **E**. Halogen bonds are marked in green as **F**. Depending on the position of the halogen bond in the theophylline molecule, these interactions are further subclassified into the types **F1**–**F3** (Figure 1). The classification of interaction types is based only on the interaction sites of the theophylline molecule rather than on a strict separation of all possible donor–acceptor combinations. For example, hydrogen bonds involving the same interaction site but different donor groups (e.g., O–H···O and N–H···O) are assigned to the same interaction category. Due to the large number of different interaction patterns possible, only the three most dominant patterns will be presented here in detail.

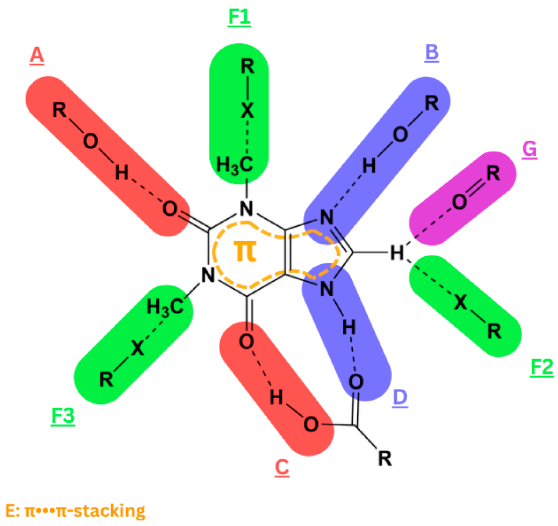

Figure 1. Illustration of the major intermolecular interactions that the theophylline molecule undergoes.

The evaluated geometric parameters were based on van der Waals criteria and defined to ensure a consistent classification and sound analysis of interactions. Thus, classical hydrogen bonds were identified using donor–acceptor atom distances in the range of 2.4 to 3.2 Å and angles between 100° and 180° [21,22]. Non-classical hydrogen bonds were characterised by hydrogen-oxygen distances of less than 2.8 Å and angles ranging from 100° to 180° [21,23]. For the identification of halogen bonds, the sum of the van der Waals radii of the interacting atoms was used as a distance criterion, with the distance derived from the corresponding crystal structure shorter than the sum of the respective van der

Waals radii [24,25]. The π···π interactions were considered within an interplanar distance of 3.0 to 4.0 Å, which corresponds to the typical distances observed for aromatic π···π stacking interactions in crystal structures. Strong interactions occur around 3.3 Å, while weaker contacts may extend to 3.8 Å, even though these values are not absolute. Only the shortest distances and angles of the observed π···π interaction were included. For the second part, a Hirshfeld surface analysis was carried out using the Crystal Explorer 21 software [3] to visualise intermolecular contacts within the three most common interaction patterns of theophylline. The resulting Hirshfeld surfaces and 2D fingerprint plots provide a graphical representation of close contacts and their relative contributions within the crystal packing. The identification of interaction motifs in this study is primarily based on geometrical criteria such as interatomic distances and angles, while the Hirshfeld analysis serves to illustrate these structural features. All fingerprint plots corresponding to the analysed interaction patterns are provided in the Supplementary Material.

3. Results and Discussion

The objective of this work is to present an analysis of the interaction behaviour of theophylline in its co-crystals. Through systematic categorization of the structures of fifty-three co-crystals with comparable co-formers, using a case-optimised interaction pattern motive (see Figure 1), three key observations have been made.

The first key observation is theophylline's versatility in its intermolecular interactions. After analysing all investigated co-crystals, twenty distinct interaction patterns have been found and various kinds of interactions at different sites can be observed: hydrogen bonds (**A**–**D**), π···π-stacking interactions (**E**), C-H···O interactions (**G**), and halogen bonds (**F1**–**F3**). Table 1 shows which interaction sites are more involved in the formation of the co-crystals. It is noteworthy that all possible interactions sites are used in the formation of the co-crystals. If one considers interactions formed at specific sites, sites **A** and **F** are under-represented. While the low number of halogen bonds (**F1**–**F3**) can be explained by the selection of only a few halogen-containing co-crystal components, the relatively low number of hydrogen bonds formed at site **A** is relevant for future observations. The absence of a strong interaction at this site suggests that the steric hindrance caused by the two adjacent methyl groups of theophylline may reduce the accessibility to this site. Thus, interactions at more sterically open interaction sites are favourable, showing that factors like steric and molecular orientation can be as influential as donor–acceptor compatibility in dictating the interaction pattern.

Table 1. Count of included interaction sites within all investigated co-crystals (53 structures). See Figure 1 for a definition of the interactions.

Interaction	A	B	C	D	E	F	G
Count	21	45	50	56	50	6	50

While these interaction sites are universally accessible in principle, their observed frequencies are influenced not only by the intrinsic interaction preferences of theophylline but also by the chemical nature of the selected co-crystal components. In particular, the dataset contains a higher proportion of structurally related aromatic carboxylic acids and short-chain compounds, which inherently favour similar hydrogen bonding and π-interaction motifs. Therefore, the reported distribution should be interpreted as a combined outcome of molecular complementarity and dataset composition.

The second key observation is that co-crystals involving theophylline are formed by various combinations of interaction patterns. A detailed table of all patterns and the number of times they occur can be found in Table 2. Theophylline forms a wide range

of twenty different interaction motifs, but the patterns vary in their frequency. There are three patterns that stand out in terms of their frequency. It should be noted that the observed frequency distribution is influenced by both the intrinsic interaction capabilities of theophylline and the chemical composition of the selected co-crystal component set.

Table 2. Summary of all interaction patterns involving the investigated theophylline co-crystals.

Code type	ABCDEG 1	ABCDE 2	ABCDG 3	ABDEG 4	ACDEG 5
Count	9	2	3	1	2
Code type	BCDEG 6	BCDE 7	BCDG 8	BDEG 9	CDEG 10
Count	15	2	1	2	5
Code type	DEG 11	ACDEF23 12	BCDEF1G 13	BCDEF23G 14	BCDF13 15
Count	1	1	1	1	1
Code type	BCDF23 16	CDEF1G 17			
Count	1	1			
Code type	ABCDEG & BCDEG 18	ABCDEG & BDEG 19		BCDEG & CDEG 20	
Count	1	2		1	

The most dominant pattern is the **BCDEG** pattern (first line, Figure 2), occurring fifteen times throughout all selected co-crystals. This pattern includes hydrogen bonds at sites **B**, **C**, **D**, and a non-classical hydrogen bond at site **G**, as well as π···π-stacking-interactions **E**. Co-crystals with aromatic carboxylic acids and short dicarboxylic chains notably belong to this group. Interaction site **A** is missing in the most dominant pattern, proving the observation made previously that site A is unfavoured for steric reasons. In particular, co-formers with aromatic carboxylic acids and short dicarboxylic chains are part of this type. The second most common pattern found is **ABCDEG** (see the middle part of Figure 2), which can be observed nine times across all investigated co-crystals. This pattern includes hydrogen bonding at all four primary positions, **A**, **B**, **C**, and **D,** and the non-classical site **G**, as well as π···π-stacking **E**. Particularly, co-crystal components that are aromatic dihydroxybenzoic acids form this interaction pattern. This example illustrates that even the less accessible site **A** can still interact with neighbouring molecules when more complex co-former molecules with many functional groups are used. To take into account all of the interaction sites involving theophylline, complex components structurally adapted to theophylline must be selected. The third most common interaction pattern is **CDEG** (first line right, Figure 2) and can be counted five times within the selected co-crystals. In this pattern, interaction sites **A** and **B** are missing. Only two classical hydrogen bonds are formed at sites **C** and **D**, and a non-classical one at site **G**, as well as π···π-stacking **E**. This interaction pattern shows that the steric hindrance of site **A** can be expanded to site **B**. Many components possess bifunctional groups, capable of acting as both a donor and acceptor. However, when site **A** is inaccessible, the full interaction potential cannot be fulfilled, leading to no interaction with site **B**. Interactions then often shift to the more accessible sites **C** and **D**. Besides the schematic illustrations, real representations are shown in Figure 3.

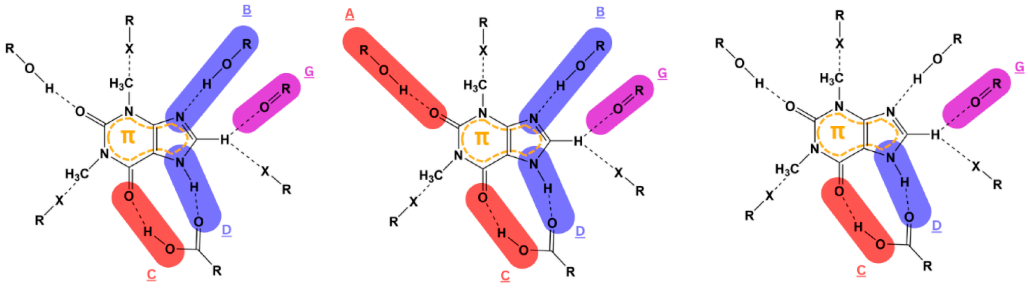

Figure 2. The most common interaction patterns of co-crystals of theophylline illustrated schematically, from left to right: BCDEG, ABCDEG and CDEG. π···π-stacking illustrated as an orange π.

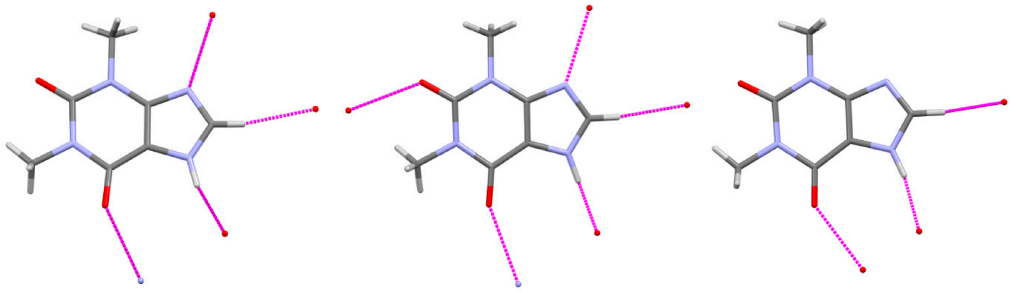

Figure 3. Theophylline's most common interaction patterns, from left to right: BCDEG, ABCDEG and CDEG.

The third key observation is the frequency of the occurrence of mutual hydrogen bonds between two theophylline molecules only at interaction sites **C** and **D**. Out of fifty-three analysed co-crystals, twenty engage in centrosymmetric N-H···O hydrogen bonds with another theophylline molecule, forming a cyclic dimer. Theophylline interacts with a neighbouring molecule to form a hydrogen bonded, thus acting both as a donor and an acceptor (see Figure 4). The fact that this dimeric motif is one of the most favourite bonding situations for theophylline, has been highlighted in other studies covering the solid-state phases of theophylline-based co-crystals [26–28]. The donor–acceptor distances and bond angles are identical for both sites. The high occurrence of this cyclic dimeric structure illustrates that if steric or electronic conditions are not met by the co-crystal component, theophylline tends to form dimeric structures on its own.

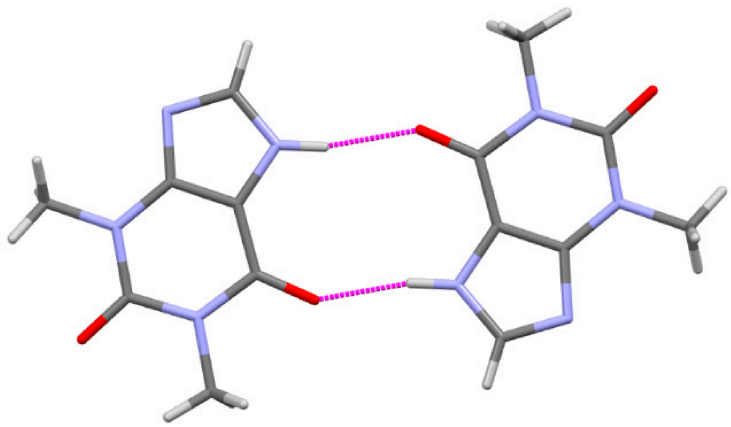

Figure 4. The formation of a cyclic dimeric theophylline structure.

The results of the 2D fingerprint plots and Hirshfeld surface analyses will now be presented. This procedure was undertaken in order to display and compare the total contributions of all relevant interactions, as well as to highlight the characteristic inter-

molecular interactions. Regarding the total contribution of all relevant interactions, for all three interaction patterns, the distribution of interactions is similar. For three patterns BCDEG, ABCDEG and CDEG, the O···H and H···H interactions make up the largest number of intermolecular interactions, followed by N···H and C···H contacts. The value for the standard deviation for the N···N interaction is higher for all three patterns than the mean value. This shows that the values for this interaction are unreliable (Table 3).

Table 3. Summary of average contributions of interactions for all investigated theophylline co-crystals for the BCDEG, ABCDEG and CDEG interaction patterns.

Interaction	**O···O**	**O···C**	**O···H**	**O···N**	**C···C**	**C···H**	**C···N**	**H···H**	**H···N**	**N···N**
Pattern	**BCDEG**									
Mean %	0.90	4.08	31.65	1.65	4.34	7.83	3.34	35.35	10.15	0.75
Std dev.	0.65	2.05	4.62	1.34	2.06	1.30	0.87	6.18	2.02	0.86
Pattern	**ABCDEG**									
Mean %	0.69	3.04	29.01	1.40	5.70	8.18	3.99	38.67	9.03	0.29
Std dev.	0.55	1.82	5.37	0.74	0.70	2.66	1.24	4.85	1.79	0.65
Pattern	**CDEG**									
Mean %	0.58	1.50	27.96	0.68	6.54	8.78	4.16	38.08	9.68	0.44
Std dev.	0.16	0.49	0.98	0.37	1.16	2.66	0.36	2.97	1.07	0.83

To investigate further which specific interactions are characteristic for each interaction pattern, the sharp spikes observed in the 2D Hirshfeld fingerprint plots were examined. Two general motifs have been observed throughout the three most common interaction patterns. It should be pointed out that these motifs do not have to be exclusive, and intermediate motifs may be present. The first motif displays two spike-containing regions, whereas the second motif is defined by three regions. Each region is showing one to two sharp spikes. The positions of the spikes further provide insight into the underlying interactions. In the fingerprint plot, the outer spikes correspond to hydrogen-bonding interactions. O-related contacts appear on both sides of the diagonal, reflecting interactions with similar atoms, while N-related contacts are mainly observed on one side, indicating interactions between theophylline molecules and the co-crystal component. Mirror symmetry, with respect to the diagonal, reflects contacts between theophylline molecules, whereas asymmetry indicates contacts with the co-crystal component. A central spike, when present, corresponds to H···H interactions. Representative examples of the two motifs are shown in Figures 5 and 6. Regarding the dominant interaction patterns, each tends to form one of the two motifs. **BCDEG** tends to form only two spike-containing regions, with few three-spike-containing regions. For **ABCDEG** it is the other way round; this interaction pattern tends to be characterised by three-spike-containing regions with only a few exceptions leaning to the two-spike-containing regions. **CDEG** clearly forms the three-spike-containing motif. The reason for the different motifs is the stabilising effect of the hydrogen bonds. While co-crystals of the **BCDEG** and **ABCDEG** patterns form three to four hydrogen bonds, the ones of the **CDEG** pattern form two hydrogen bonds, so they can only be stabilised by forming weak but highly characteristic H···H interactions, represented in the middle spike region. Lastly, many co-crystals with the **ABCDEG** pattern do not exhibit their four hydrogen bonds in the fingerprint analysis. While, theoretically, four spikes should be seen for all four hydrogen bonds, often only three are visible. This could be due to two different reasons. It could be that even though software such as the Mercury (Ver. 4.0) programme identifies four hydrogen bonds with acceptor–donor distances and angles in the allowable ranges, one of these interactions, probably the one at site **A**, exhibits comparatively longer intermolecular distances. It should be noted that fingerprint plots are derived purely from

geometrical parameters. Therefore, the prominence of a spike does not directly reflect interaction strength, but rather the corresponding intermolecular distances. If a hydrogen bond approaches or exceeds the sum of the respective van der Waals radii, the associated d_i and d_e values will not produce a pronounced spike in the fingerprint plot. Alternatively, two spikes could lay on top of each other, making it difficult to differentiate between both.

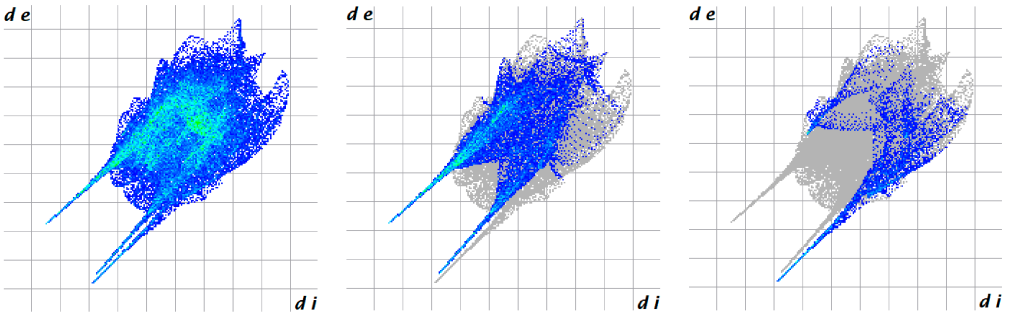

Figure 5. Hirshfeld 2D fingerprint plots of the theophylline-malonic acid co-crystal, from left to right: all interactions, O···H interactions, N···H interactions.

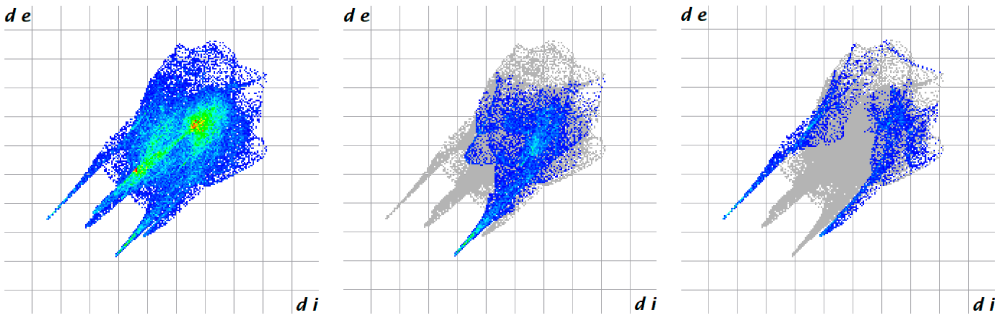

Figure 6. Hirshfeld 2D fingerprint plots of the theophylline-pyridine-2,6-diamino acid co-crystal, from left to right: all interactions, O···H interactions, N···H interactions.

4. Conclusions and Outlook

Theophylline has been analysed in this work by investigating the specific interaction sites involved in the formation of co-crystals with different components, followed by a Hirshfeld surface analysis based on deposited structures with the Crystal Structure Database. Theophylline possesses various interaction sites and can form interactions at each one, but interaction site **A** is an exception. Less than half of all selected co-crystals form strong interactions at this site. The reason for this can be found in the sterically unfavourable position of site **A** between two methyl groups. Consequently, the most common interaction pattern found is **BCDEG**, leaving out interaction site **A**. The **ABCDEG** and **CDEG** interaction patterns follows as the second and third most common interaction patterns. A key observation is the formation of dimeric cyclic units, where two theophylline molecules engage in two centrosymmetric N-H···O hydrogen bonds at interaction sites **C** and **D**, confirming the previous observation for pure theophylline [13,26–28]. Lastly, Hirshfeld surface analyses have been created for the three most common interactions patterns. It is apparent that each interaction pattern exhibits similar Hirshfeld surfaces with characteristic sharp spikes in the 2D fingerprint plots. Nevertheless, there are various degrees of intermediate motifs, making it difficult to clearly classify co-crystals. Concerning the contribution of all various interactions to the formation of the co-crystal, no strong differences have been observed. Finally, it should be noted that the possible maximum number of hydrogen bonds for the **ABCDEG** pattern, after analysing with the software Mercury (Ver. 4.0), did not correspond to the number of characteristic interactions visible in the Hirshfeld 2D fingerprint analysis.

A systematic analysis of substance profiles for molecular compounds and their co-crystals is of great importance for achieving a deeper understanding of the intermolecular interaction behaviour and has potential for crystal engineering. However, extracting and analysing all relevant structural and interaction data is often time-consuming. In this context, artificial intelligence-based approaches provide an interesting new perspective, as they promise to enable the rapid analysis of complex datasets, possibly helping in the future to create reliable and informative substance profiles. In the future, automated, potentially AI-supported analysis will be used to perform more detailed quantum-chemistry-based studies on larger groups of similar structures to determine the energetic contributions of each interaction [13], and in the best case, high quality structures that are, for example refined using non-spherical atomic form factors [29]. Nevertheless, a preliminary selection process will most probably still be required.

Supplementary Materials: The following supporting information can be downloaded at https://www.mdpi.com/article/10.3390/cryst16050342/s1, Crystallographic Supplementary Material, which includes all references of the analysed structures.

Author Contributions: Conceptualization, G.J.R.; Software, M.H.P.; Validation, M.H.P.; Formal analysis, G.J.R.; Data curation, M.H.P. and G.J.R.; Writing—original draft, M.H.P.; Writing—review and editing, G.J.R.; Visualisation, M.H.P. and G.J.R.; Supervision, G.J.R. All authors have read and agreed to the published version of the manuscript.

Funding: This research received no external funding.

Data Availability Statement: In this work, a substance profile is established with a structure and a level of detail that has not previously been reported in this form. The systematic approach applied was inspired by earlier work by Bučar et al. [19] and Corpinot et al. [20] and others, where the interaction profile of theophylline co-crystals was illustrated and categorised in a similar way. However, the methodology presented in this study has been significant expanded, refined, and optimised to provide a more structured framework. In contrast to the aforementioned articles, we comparatively analysed a large number of structures taken from the structural database. The original contributions presented in this study are included in the article/Supplementary Material. Further inquiries can be directed to the corresponding author.

Acknowledgments: The authors would like to thank Richard Goddard for fruitful discussions and his valuable insights into the structural chemistry aspects of this work.

Conflicts of Interest: The authors declare no conflict of interest.

References

1. Galanakis, N.; Tuckerman, M.E. Rapid prediction of molecular crystal structures using simple topological and physical descriptors. *Nat. Commun.* **2024**, *15*, 9757. [CrossRef]
2. Price, S.L. Molecular crystal structure prediction. In *Molecular Crystal Structure Prediction*; Elsevier: Amsterdam, The Netherlands, 2018.
3. Spackman, P.R.; Turner, M.J.; McKinnon, J.J.; Wolff, S.K.; Grimwood, D.J.; Jayatilaka, D.; Spackman, M.A. CrystalExplorer: A program for Hirshfeld surface analysis, visualization and quantitative analysis of molecular crystals. *J. Appl. Crystallogr.* **2021**, *54*, 1006–1011. [CrossRef]
4. Aakeröy, C.B.; Salmon, D.J. Building co-crystals with molecular sense and supramolecular sensibility. *CrystEngComm* **2005**, *7*, 439–448. [CrossRef]
5. Vishweshwar, P.; McMahon, J.A.; Bis, J.A.; Zaworotko, M.J. Pharmaceutical co-crystals. *J. Pharm. Sci.* **2006**, *95*, 499–516. [CrossRef]
6. Schultheiss, N.; Newman, A. Pharmaceutical cocrystals and their physicochemical properties. *Cryst. Growth Des.* **2009**, *9*, 2950–2967. [CrossRef]
7. Jia, Y.; Yang, D.; Wang, W.; Hu, K.; Yan, M.; Zhang, L.; Gao, L.; Lu, Y. Recent advances in pharmaceutical cocrystals of theophylline. *Nat. Prod. Bioprospect.* **2014**, *14*, 53. [CrossRef]
8. Liu, H.; Chan, H.C.S.; Yu, X.; Li, J.; Li, J.; Zhou, Z. Two polymorphic cocrystals of theophylline with ferulic acid. *Cryst. Growth Des.* **2023**, *23*, 4448–4459. [CrossRef]

9. Bhowmik, A.; Bamane, S.; Saxena, A.K.; Mishra, M.K. Caffeine vs. theophylline cocrystals: Insights into structure–mechanical behavior and piezoelectricity. *Cryst. Growth Des.* **2025**, *25*, 5007–5021. [CrossRef]
10. Stanton, S.A.; Du, J.J.; Lai, F.; Stanton, G.; Hawkins, B.A.; Ong, J.A.; Groundwater, P.W.; Platts, J.A.; Hibbs, D.E. Understanding hygroscopicity of theophylline via a novel cocrystal polymorph: A charge density study. *J. Phys. Chem. A* **2021**, *125*, 9736–9756. [CrossRef]
11. Domingos, F.N.B.; de Oliveira Neto, J.G.; Souto, E.B.; Ayala, A.P.; Araújo, B.S.; Ferreira, A.A.; Nogueira, C.E.S.; dos Santos, A.O. From crystal design to pharmaceutical drug potential: A new theophylline-nitrate monohydrate cocrystal salt with enhanced solubility and antibacterial activity. *Cryst. Growth Des.* **2026**, *26*, 2068–2080. [CrossRef]
12. Tu, Y.; Chen, S.; Liu, X.; Yuan, S.; Zhou, Y.; Yang, J.; Qian, K.; Cheng, L. Enhancing solubility and antioxidant properties: Synthesis and characterization of kaempferol-theophylline cocrystal. *J. Drug Deliv. Sci. Technol.* **2025**, *113*, 107334. [CrossRef]
13. Konovalova, I.S.; Shishkina, S.V.; Wyshusek, M.; Patzer, M.; Reiss, G.J. Supramolecular architecture of theophylline polymorphs, monohydrate and co-crystals with iodine: Study from the energetic viewpoint. *RSC Adv.* **2024**, *14*, 29774–29788. [CrossRef]
14. Reiss, G.J. A cyclic I_{10}^{2-} anion in the layered crystal structure of theophyllinium pentaiodide, $C_7H_9I_5N_4O_2$. *Z. Krist. New Cryst. Struct.* **2019**, *234*, 737–739. [CrossRef]
15. Reiss, G.J.; Wyshusek, M.; Rheinländer, J.C.; Konovalova, I.S. Hydrogen bonding and $\pi\cdots$halogen interactions in the crystal structure of bis(theophyllinium) hexachloridoplatinate(IV) monohydrate. *Z. Krist. New Cryst. Struct.* **2024**, *239*, 813–816. [CrossRef]
16. Merkelbach, J.; Majewski, M.A.; Reiss, G.J. Crystal structure of caffeinium triiodide–caffeine (1/1). *Z. Krist. New Cryst. Struct.* **2018**, *233*, 941–944. [CrossRef]
17. Cambridge Crystallographic Data Centre. Available online: https://www.ccdc.cam.ac.uk (accessed on 18 March 2026).
18. Macrae, C.F.; Sovago, I.; Cottrell, S.J.; Galek, P.T.; McCabe, P.; Pidcock, E.; Platings, M.; Shields, G.P.; Stevens, J.S.; Towler, M.; et al. Mercury 4.0: From visualization to analysis, design and prediction. *J. Appl. Crystallogr.* **2020**, *53*, 226–235. [CrossRef]
19. Bucar, D.K.; Henry, R.F.; Zhang, G.G.; MacGillivray, L.R. Synthon hierarchies in crystal forms composed of theophylline and hydroxybenzoic acids: Cocrystal screening via solution-mediated phase transformation. *Cryst. Growth Des.* **2014**, *14*, 5318–5328. [CrossRef]
20. Corpinot, M.K.; Stratford, S.A.; Arhangelskis, M.; Anka-Lufford, J.; Halasz, I.; Judaš, N.; Jones, W.; Bučar, D.K. On the predictability of supramolecular interactions in molecular cocrystals -The view from the bench. *CrystEngComm* **2016**, *18*, 5434–5439. [CrossRef]
21. Brown, I.D. On the geometry of O–H$\cdots$O hydrogen bonds. *Acta Crystallogr. A* **1976**, *32*, 24–31. [CrossRef]
22. Desiraju, G.R.; Steiner, T. *The Weak Hydrogen Bond: In Structural Chemistry and Biology*; Oxford University Press: Oxford, UK, 2001.
23. Johnston, R.C.; Cheong, P.H.-Y. C–H$\cdots$O non-classical hydrogen bonding in the stereomechanics of organic transformations: Theory and recognition. *Org. Biomol. Chem.* **2013**, *11*, 5057–5064. [CrossRef]
24. Auffinger, P.; Hays, F.A.; Westhof, E.; Ho, P.S. Halogen bonds in biological molecules. *Proc. Natl. Acad. Sci. USA* **2004**, *101*, 16789–16794. [CrossRef]
25. Hu, S.-Z.; Zhou, Z.H.; Xie, Z.X.; Robertson, B.E. A comparative study of crystallographic van der Waals radii. *Z. Krist. Cryst. Mater.* **2014**, *229*, 517–523. [CrossRef]
26. Kakkar, S.; Bhattacharya, B.; Reddy, C.M.; Ghosh, S. Tuning mechanical behaviour by controlling the structure of a series of theophylline co-crystals. *CrystEngComm* **2018**, *20*, 1101–1109. [CrossRef]
27. Khamar, D.; Pritchard, R.G.; Bradshaw, I.J.; Hutcheon, G.A.; Seton, L. Polymorphs of anhydrous theophylline: Stable form IV consists of dimer pairs and metastable form I consists of hydrogen-bonded chains. *Acta Crystallogr.* **2011**, *C67*, o496–o499. [CrossRef]
28. McTague, H.; Rasmuson, Å.C. Nucleation in the theophylline/glutaric acid cocrystal system. *Cryst. Growth Des.* **2021**, *21*, 3967–3980. [CrossRef]
29. Konovalova, I.S.; Nöthling, N.; Reiss, G.J. Energetic perspective on the crystal structure organization principles of meta-halogen-substituted anilines. *J. Mol. Struct.* **2026**, *1349*, 143745. [CrossRef]